Synthesis and Reactivity of the 9- and 10-Vertex Iron−Monocarborane Anions [7,7,7-(CO)$_3$-*closo*-7,1-FeCB$_7$H$_8$]$^-$ and [6,6,6,10,10,10-(CO)$_6$-*closo*-6,10,1-Fe$_2$CB$_7$H$_8$]$^-$

Andreas Franken, Thomas D. McGrath, and F. Gordon A. Stone*

Department of Chemistry & Biochemistry, Baylor University, Waco, Texas 76798-7348

Received July 12, 2005

The reagent [NBu$^n_4$][*closo*-1-CB$_7$H$_8$] reacts with [Fe$_3$(CO)$_{12}$] in THF at reflux temperatures to give the anion [7,7,7-(CO)$_3$-*closo*-7,1-FeCB$_7$H$_8$]$^-$, isolated as the [N(PPh$_3$)$_2$]$^+$ salt (**1a**). Further heating with excess [Fe$_3$(CO)$_{12}$] inserts a second {Fe(CO)$_3$} fragment to yield [6,6,6,10,10,10-(CO)$_6$-*closo*-6,10,1-Fe$_2$CB$_7$H$_8$]$^-$, also isolated as its [N(PPh$_3$)$_2$]$^+$ salt (**2**). Compounds **1a** and **2** react with [CuCl(PPh$_3$)]$_4$ and Tl[PF$_6$] to yield the bi- and trimetallic complexes [6,7,9-{Cu(PPh$_3$)}-6,9-(μ-H)$_2$-7,7,7-(CO)$_3$-*closo*-7,1-FeCB$_7$H$_6$] (**4**) and [7,10-{Cu(PPh$_3$)}-7-(μ-H)-6,6,6,10,10,10-(CO)$_6$-*closo*-6,10,1-Fe$_2$CB$_7$H$_7$] (**5**), respectively. Compound **2** with Ag[PF$_6$] and PPh$_3$ fails to give the analogous Ag−Fe$_2$CB$_7$ species, but instead under oxidative conditions one {Fe(CO)$_3$} moiety is removed from the anion of **2** and the anion of **1a** is isolated as the [Ag(PPh$_3$)$_3$]$^+$ salt (**1b**). The bimetallic species [6,7,9-{Ag(PPh$_3$)}-6,9-(μ-H)$_2$-7,7,7-(CO)$_3$-*closo*-7,1-FeCB$_7$H$_6$] (**6**) is also obtained. Treatment of **2** with CF$_3$SO$_3$H in donor solvents L yields the zwitterionic B-substituted compounds [6,6,6,10,10,10-(CO)$_6$-7-L-*closo*-6,10,1-Fe$_2$CB$_7$H$_7$] (L = SMe$_2$ (**7**), THF (**8**)). The former of these products reacts with SMe$_2$ in the presence of Me$_3$NO to yield the doubly substituted species [6,6,10,10,10-(CO)$_5$-6,7-(SMe$_2$)$_2$-*closo*-6,10,1-Fe$_2$CB$_7$H$_7$] (**9**), while the latter with the nucleophile PEt$_3$ undergoes THF ring opening to yield [6,6,6,10,10,10-(CO)$_6$-7-{O(CH$_2$)$_4$PEt$_3$}-*closo*-6,10,1-Fe$_2$CB$_7$H$_7$] (**12**).

Introduction

The chemistry of transition-metal complexes derived from smaller monocarborane cages such as [*closo*-1-CB$_7$H$_8$]$^-$ has hitherto received very little attention, due to the fact that until recently the syntheses of the smaller monocarboranes were tedious and afforded only poor yields.[1] On the other hand, a range of dicarboranes C$_2$B$_n$H$_{n+2}$ (n = 6−10) of various cluster sizes has been far more easily accessible for over three decades.[2] Direct insertion of d^{10} Ni, Pd, and Pt species into 8-, 9-, and 11-atom *closo*-dicarborane cages is therefore well-known, and reports of this appeared in the literature around 30 years ago.[3] There have been only a few examples in the literature of smaller monocarborane complexes of transition metals. One of the first examples was the 9-vertex anion [7-(η^5-C$_5$H$_5$)-*closo*-7,1-CoCB$_7$H$_8$]$^-$ synthesized by Hawthorne and co-workers[4] via a polyhedral contraction reaction involving base degradation of 13-vertex [4-(η^5-C$_5$H$_5$)-*closo*-4,1,6-CoC$_2$B$_{10}$H$_{12}$]. Approximately two decades later Kennedy and co-workers[5] treated [IrCl(CO)(PPh$_3$)$_2$] with the [*closo*-1-CB$_7$H$_8$]$^-$ anion in an oxidative-insertion type of reaction to yield the 9-vertex species [7-CO-7,7-(PPh$_3$)$_2$-*closo*-7,1-IrCB$_7$H$_8$]. The recent discovery of Brellochs[6] that formaldehyde reacts with B$_{10}$H$_{14}$ in strongly alkaline solution to yield the [*arachno*-6-CB$_9$H$_{14}$]$^-$ anion and that similar reactions with a variety of other aldehydes also give {CB$_9$} monocarboranes, led to an easy entry into complete series of smaller monocarborane anions.[7] These findings complement and significantly expand the repertoire of synthetic routes to monocarboranes.[2a,8] Eight-vertex [*closo*-1-CB$_7$H$_8$]$^-$ is now readily available in amounts that allow exploration of its further chemistry with

* To whom correspondence should be addressed. E-mail: gordon_stone@baylor.edu.

(1) Plesek, J.; Jelínek, T.; Stíbr, B.; Hermánek, S. *J. Chem. Soc., Chem. Commun*. **1988**, 348.

(2) (a) Stíbr, B. *Chem. Rev.* **1992**, *92*, 225. (b) Bregadze, V. I. *Chem. Rev.* **1992**, *92*, 209.

(3) (a) Green, M.; Howard, J. A. K.; Spencer, J. L.; Stone, F. G. A. *J. Chem. Soc., Chem. Commun*. **1974**, 153. (b) Green, M.; Spencer, J. L.; Stone, F. G. A.; Welch, A. J. *J. Chem. Soc., Chem. Commun*. **1974**, 571. (c) Green, M.; Spencer, J. L.; Stone, F. G. A.; Welch, A. J. *J. Chem. Soc., Chem. Commun*. **1974**, *794*. (d) Green, M.; Spencer, J. L.; Stone, F. G. A.; Welch, A. J. *J. Chem. Soc., Dalton Trans.* **1975**, 179. (e) Barker, G. K.; Green, M.; Spencer, J. L.; Stone, F. G. A.; Taylor, B. F.; Welch, A. J. *J. Chem. Soc., Chem. Commun*. **1975**, 804. (f) Carroll, W. E.; Green, M.; Stone, F. G. A.; Welch, A. J. *J. Chem. Soc., Dalton Trans*. **1975**, 2263. (g) Green, M.; Howard, J. A. K.; Spencer, J. L.; Stone, F. G. A. *J. Chem. Soc., Dalton Trans*. **1975**, 2278. (h) Barker, G. K.; Green, M.; Onak, T. P.; Stone, F. G. A.; Ungermann, C. B.; Welch, A. J. *J. Chem. Soc., Chem. Commun*. **1978**, 169. (i) Green, M.; Spencer, J. L.; Stone, F. G. A. *J. Chem. Soc., Dalton Trans*. **1979**, 1679. (j) Barker, G. K.; Green, M.; Stone, F. G. A. *J. Chem. Soc., Dalton Trans*. **1980**, 1186. (k) Barker, G. K.; Green, M.; Stone, F. G. A.; Welch A. J.; Wolsey, W. C. *J. Chem. Soc., Chem. Commun*. **1980**, 627.

(4) Dustin, D. F.; Hawthorne, M. F. *Inorg. Chem.* **1973**, *12*, 1380.

(5) Stíbr, B.; Kennedy, J. D.; Thornton-Pett, M.; Drdáková, E.; Jelínek, T.; Plesek, J. *Collect. Czech. Chem. Commun*. **1992**, *57*, 1439.

(6) Brellochs, B. In *Contemporary Boron Chemistry*; Davidson, M. G., Hughes, A. K., Marder, T. B., Wade, K., Eds.; Royal Society of Chemistry: Cambridge, U.K., 2000; p 212.

(7) (a) Stíbr, B. *Pure Appl. Chem.* **2003**, *75*, 1295. (b) Brellochs, B.; Backovsky, J.; Stíbr, B.; Jelínek, T.; Holub, J.; Bakardjiev, M.; Hnyk, D.; Hofmann, M.; Císarová, I.; Wrackmeyer, B. *Eur. J. Inorg. Chem*. **2004**, 3605. See also: Franken, A.; Kilner, C. A.; Thornton-Pett, M.; Kennedy, J. D. *Collect. Czech. Chem. Commun*. **2002**, *67*, 869. Jelínek, T.; Thornton-Pett, M.; Kennedy, J. D. *Collect. Czech. Chem. Commun*. **2002**, *67*, 1035.

10.1021/om050584j CCC: $30.25
Publication on Web 09/10/2005

Chart 1

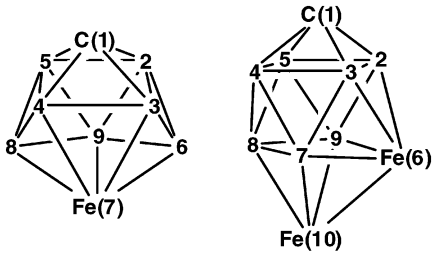

transition-metal reagents, an area that we are actively investigating. We here report the first fruits of these studies, namely the products of the reaction of this carborane with iron carbonyls.

Results and Discussion

When $[Fe_3(CO)_{12}]$ and $[NBu^n_4][closo\text{-}1\text{-}CB_7H_8]$ are heated to reflux in THF for 5 h, the anionic complex $[7,7,7\text{-}(CO)_3\text{-}closo\text{-}7,1\text{-}FeCB_7H_8]^-$ is formed and, following addition of $[N(PPh_3)_2]Cl$, is conveniently isolated as the $[N(PPh_3)_2]^+$ salt (**1a**) (Chart 2). (Vertexes for the compounds discussed herein are numbered as in Chart 1.) The preparation of this ferracarborane anion can be regarded as an oxidative insertion of Fe(0) into the cluster, formally generating an Fe(II) center and an effectively η^5 tridentate $\{nido\text{-}CB_7H_8\}^{3-}$ ligand by concomitant reduction of the $\{closo\text{-}CB_7H_8\}^-$ starting substrate. Further heating of the reaction mixture (18 h total) in the presence of excess $[Fe_3(CO)_{12}]$ converts the anion of **1a** to the anionic diiron complex $[6,6,6,10,10,10\text{-}(CO)_6\text{-}closo\text{-}6,10,1\text{-}Fe_2CB_7H_8]^-$, which may similarly also be isolated as its $[N(PPh_3)_2]^+$ salt (**2**). This reaction can be regarded as a second oxidative insertion of Fe(0) into the anion of **1a**. At this stage, further insertion of Fe(0) into the closo 10-vertex $\{Fe_2CB_7\}$ cluster becomes unlikely, because of the kinetic stability of the 10-vertex metallamonocarborane cluster.[9] The salts **1a** and **2** are purified by column chromatography and are sufficiently pure for further reactions.

As the compounds **1a** and **2** are precursors to other complexes, structural studies on both ferracarboranes were merited. In the case of the former, suitable crystals were available of the $[Ag(PPh_3)_3]^+$ salt **1b** (see below). The structures of the anions of compounds **1b** and **2** are shown in Figure 1. The cluster of **1b** reveals a partial opening that is apparently characteristic of many other formally closo 9-vertex clusters.[5,10,11] All such species structurally examined so far have at least one interboron distance that is toward the longer end of typical cluster B−B connectivities (ca. >1.9 Å), and generally there is at least one B···B separation that is over 2 Å, an arbitrary value that can be chosen as a weak-bonding limit. In **1b** this lengthening is seen between B(3) and B(4) (2.137(3) Å).

The two iron vertexes in **2** cause the 10-vertex cluster geometry to be slightly distorted with Fe(6)−Fe(10) = 2.5512(4) Å. There is also an extension of the upper B−B connectivity that subtends Fe(6) (B(2)···B(3) = 1.996(2) Å). Typically in carborane and metallacarborane clusters, the electronegative carbon atom favors the least connected vertex.[12] The tendency of transition-metal atoms preferentially to occupy higher coordinate sites in metalla(hetero)boranes is also well established,[13] there being as far as we are aware only one apparent exception.[14] As Figure 1 clearly shows, the carbon vertex in **1b** and **2** occupies a 4-coordinate site, while the iron atom is in a 5-coordinate position in the 9-vertex ferracarborane of **1b**. On the other hand, the two iron atoms in **2** adopt two different types of coordination sites (4- and 5-connected) in the 10-vertex diferracarborane.

With the carbon vertex reasonably assumed always to take up the 4-connected site in a closed Fe_2CB_7 cluster having the typical bicapped-square-antiprismatic architecture, there are several possible isomers in which

Chart 2

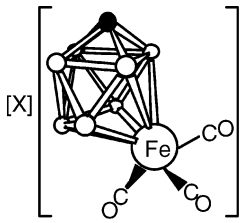

X

1a $[N(PPh_3)_2]$
1b $[Ag(PPh_3)_3]$

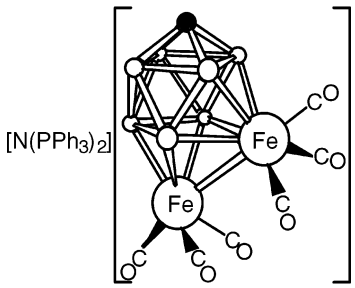

2

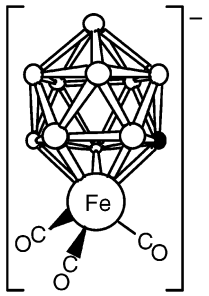

3

○ BH ● CH

(8) (a) Franken, A.; King, B. T.; Rudolph, J.; Rao, P.; Noll, B. C.; Michl, J. *Collect. Czech. Chem. Commun.* **2001**, *66*, 1238. (b) Laromaine, A.; Teixidor, F.; Viñas, C. *Angew. Chem., Int. Ed.* **2005**, *44*, 2220.

(9) Schleyer, P. v. R.; Najafian, K. *Inorg. Chem.* **1998**, *37*, 3454.

(10) Koetzle, T. F.; Scarbrough, F. E.; Lipscomb, W. N. *Inorg. Chem.* **1968**, *7*, 1076.

(11) O'Neill, M.E.; Wade, K. *Polyhedron* **1983**, *2*, 963.

(12) (a) Williams, R. E. *Adv. Inorg. Chem. Radiochem.* **1976**, *18*, 67. (b) Ott, J. J.; Gimarc, B. M. *J. Am. Chem. Soc.* **1986**, *108*, 4303.

(13) For example: Miller, V. R.; Sneddon, L. G.; Beer, D. C.; Grimes, R. N. *J. Am. Chem. Soc.* **1974**, *96*, 3090.

(14) Evans, J. W.; Dunks, G. B.; Hawthorne, M. F. *J. Am. Chem. Soc.* **1973**, *95*, 4565.

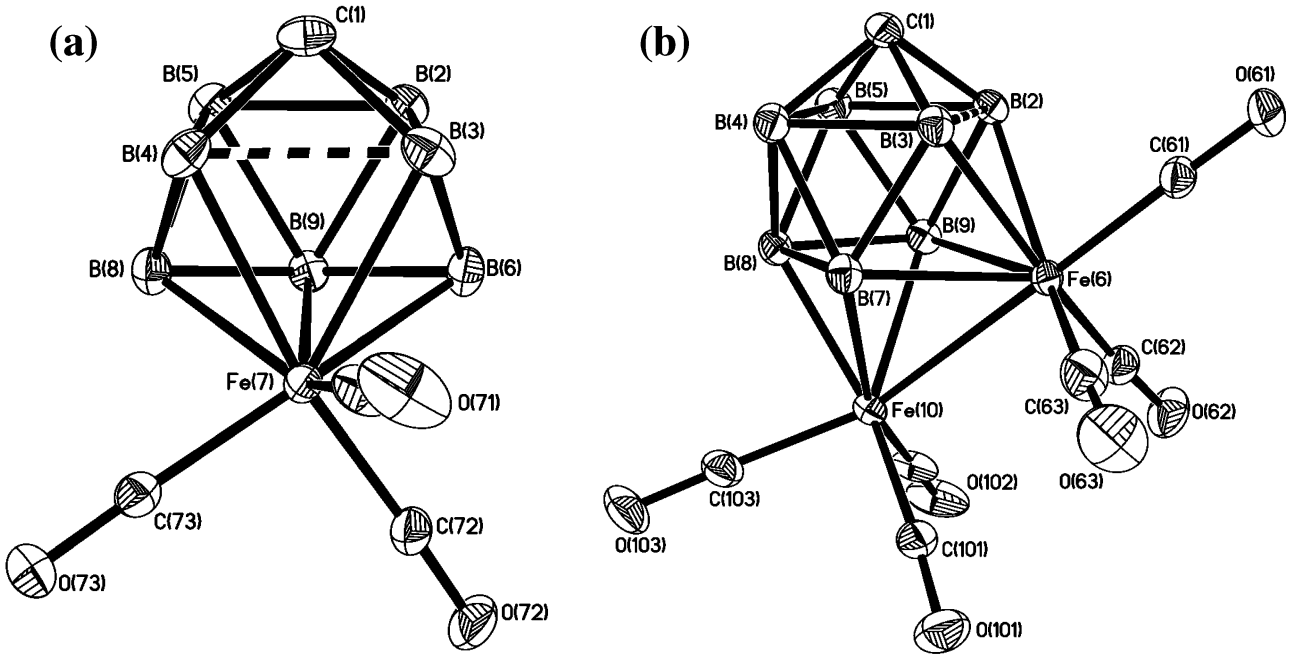

Figure 1. Perspective views of the anions of compounds (a) **1b** and (b) **2**, showing the crystallographic labeling scheme. In this and subsequent figures, thermal ellipsoids are drawn with 40% probability, and for clarity only chemically significant hydrogen atoms and (where appropriate) only the ipso carbon atoms of phenyl rings are shown. Selected internuclear distances (Å) are as follows. For **1b**: Fe(7)−B(3) = 2.3273(18), Fe(7)−B(4) = 2.2851(18), Fe(7)−B(6) = 2.1017(17), Fe(7)−B(8) = 2.0754(17), Fe(7)−B(9) = 2.2443(17), Fe(7)−C(71) = 1.7771(17), Fe(7)−C(72) = 1.7883(16), Fe(7)−C(73) = 1.7764(16), B(3)···B(4) = 2.137(3). For **2**: Fe(6)−Fe(10) = 2.5512(4), Fe(6)−B(2) = 2.1792(17), Fe(6)−B(3) = 2.1757(17), Fe(6)−B(7) = 2.2494(17), Fe(6)−B(9) = 2.2390(17), B(2)···B(3) = 1.996(2), Fe(6)−C(61) = 1.7678(16), Fe(6)−C(62) = 1.7910(17), Fe(6)−C(63) = 1.7927(18), Fe(10)−B(7) = 2.1647(16), Fe(10)−B(8) = 2.0809(17), Fe(10)−B(9) = 2.2054(17), Fe(10)−C(101) = 1.7850(17), Fe(10)−C(102) = 1.7816(17), Fe(10)−C(103) = 1.7638(17).

Table 1. Analytical and Physical Data

compd	color	yield (%)	ν_{max}(CO)[a] (cm^{-1})	anal.[b] (%) C	anal.[b] (%) H
$[N(PPh_3)_2][7,7,7\text{-}(CO)_3\text{-}closo\text{-}7,1\text{-}FeCB_7H_8]$ (**1a**)	orange	32	2021 s, 1952 s	60.9[c] (60.6)	5.0 (5.1)
$[N(PPh_3)_2][6,6,6,10,10,10\text{-}(CO)_6\text{-}closo\text{-}6,10,1\text{-}Fe_2CB_7H_8]$ (**2**)	red	63	2045 s, 2001 s, 1972 s	56.3 (56.5)	4.3 (4.2)
$[6,7,9\text{-}\{Cu(PPh_3)\}\text{-}6,9\text{-}(\mu\text{-}H)_2\text{-}7,7,7\text{-}(CO)_3\text{-}closo\text{-}7,1\text{-}FeCB_7H_6]$ (**4**)	orange	78	2045 s, 1991 s	42.8[d] (42.7)	4.2 (3.9)
$[7,10\text{-}\{Cu(PPh_3)\}\text{-}7\text{-}(\mu\text{-}H)\text{-}6,6,6,10,10,10\text{-}(CO)_6\text{-}closo\text{-}6,10,1\text{-}Fe_2CB_7H_7]$ (**5**)	red	82	2063 s, 2023 s, 2000 s, 1958 w	43.2 (42.7)	3.4 (3.3)
$[6,7,9\text{-}\{Ag(PPh_3)\}\text{-}6,9\text{-}(\mu\text{-}H)_2\text{-}7,7,7\text{-}(CO)_3\text{-}closo\text{-}7,1\text{-}FeCB_7H_6]$ (**6**)	orange	58	2043 s, 1985 s	43.6 (43.6)	3.7 (3.8)
$[6,6,6,10,10,10\text{-}(CO)_6\text{-}7\text{-}SMe_2\text{-}closo\text{-}6,10,1\text{-}Fe_2CB_7H_7]$ (**7**)	orange	79	2063 s, 2023 s, 1996 s	23.3[d] (23.0)	3.0 (3.0)
$[6,6,6,10,10,10\text{-}(CO)_6\text{-}7\text{-}\{O(CH_2)_4\}\text{-}closo\text{-}6,10,1\text{-}Fe_2CB_7H_7]$ (**8**)	orange	72	2062 s, 2044 w, 2021 s, 1991 s	26.0[e] (26.2)	3.4 (3.2)
$[6,6,10,10,10\text{-}(CO)_5\text{-}6,7\text{-}(SMe_2)_2\text{-}closo\text{-}6,10,1\text{-}Fe_2CB_7H_7]$ (**9**)	red	63	2030 s, 1978 s, 1963 s	25.4 (25.5)	4.0 (4.1)
$[6,6,6,10,10,10\text{-}(CO)_6\text{-}7\text{-}\{O(CH_2)_4PEt_3\}\text{-}closo\text{-}6,10,1\text{-}Fe_2CB_7H_7]$ (**12**)	red	83	2044 s, 1998 s, 1969 s	35.8 (36.1)	5.6 (5.4)

[a] Measured in CH_2Cl_2. A broad, medium-intensity band observed at ca. 2500−2550 cm^{-1} in the spectra of all compounds is due to B−H absorptions. [b] Calculated values are given in parentheses. In addition, N: for **1a**, 1.8 (1.8); for **2**, 1.5 (1.5). [c] Cocrystallizes with 1 molar equiv of H_2O. [d] Cocrystallizes with 1 molar equiv of CH_2Cl_2. [e] Cocrystallizes with 1.5 molar equiv of CH_2Cl_2.

the two Fe centers may or may not be mutually adjacent. The formation of the cluster of **2** as only one isomer (6,10,1-Fe_2CB_7), with the metal atoms adjacent, implies a stabilizing factor, possibly the presence of a direct Fe−Fe bond. No other isomers were observed in ^{11}B NMR analysis of the reaction mixture, although conceivably where different isomers are initially formed these readily rearrange to that observed. Equally, the precise constitution of the cluster in **2** may be a consequence of the mechanism by which it is formed from the anion of **1**. It is also notable that compound **2**, dissolved in toluene and heated to reflux for several hours, showed no rearrangement to other perhaps thermodynamically more stable cluster systems. The experiment was monitored by ^{11}B NMR and **2** was recovered unchanged. Thus, despite the supposition that both iron atoms might prefer five-coordinate sites, no rearrangement to (for example) 6,7,1- or 6,8,1-Fe_2CB_7 isomers is observed.

Spectroscopic data for compounds **1a** and **2** (Tables 1−3) are entirely consistent with the solid-state structures. In their IR spectra strong CO stretching bands are observed at 2021 and 1952 cm^{-1} (**1a**) and at 2045, 2001, and 1972 cm^{-1} (**2**). The highest of these values are almost 40 and 20 cm^{-1} lower, respectively, than those observed for the icosahedral anion $[2,2,2\text{-}(CO)_3\text{-}closo\text{-}2,1\text{-}FeCB_{10}H_{11}]^-$ (**3**),[15] and studies on the latter showed that replacement of the CO groups by other donor molecules was only possible when Me_3NO was

(15) Ellis, D. D.; Franken, A.; Jelliss, P. A.; Stone, F. G. A.; Yu, P.-Y. *Organometallics* **2000**, *19*, 1993.

Table 2. ^{1}H and ^{13}C NMR Data[a]

compd	chem shift	
	^{1}H[b]	^{13}C[c]
1a	7.65−7.47 (m, 30H, Ph), 3.68 (br s, 1H, cage CH)	215.3 (CO), 133.8−126.5 (Ph), 32.3 (br, cage C)
2	7.68−7.46 (m, 30H, Ph), 7.06 (br s, 1H, cage CH)	214.5 (CO), 213.8 (CO), 136.2−126.8 (Ph), 105.2 (br, cage C)
4	7.52−7.24 (m, 15H, Ph), 3.74 (br s, 1H, cage CH)	209.0 (CO), 133.8−128.6 (Ph), 29.7 (br, cage C)
5	7.71−7.53 (m, 15H, Ph), 6.18 (br s, 1H, cage CH)	213.4 (CO), 209.3 (CO), 133.7−128.7 (Ph), 111.7 (br, cage C)
6	7.48−7.45 (m, 15H, Ph), 3.65 (br s, 1H, cage CH)	209.7 (CO), 133.9−128.9 (Ph), 36.7 (br, cage C)
7	7.21 (br s, 1H, cage CH), 2.15 (s, 3H, Me), 2.08 (s, 3H, Me)	211.1 (CO), 210.1 (CO), 105.3 (br, cage C), 29.2 (Me), 27.0 (Me)
8	6.88 (br s, 1H, cage CH), 3.67 (br, 4H, OCH_2), 1.81 (br, 4H, OCH_2CH_2)	211.8 (CO), 210.7 (CO), 100.2 (br, cage C), 82.9 (OCH_2), 25.0 (CH_2)
9	6.90 (s, 1H, cage CH), 2.05 (s, 3H, Me), 1.97 (s, 3H, Me), 1.80 (s, 3H, Me), 1.54 (s, 3H, Me)	216.2 (CO), 213.9 (CO), 213.8 (CO), 213.7 (2 × CO), 102.4 (br, cage C), 29.2 (Me), 26.8 (Me), 26.2 (Me)
10	7.20 (br s, 1H, cage CH), 2.04 (s, 6H, SMe), 1.85 (m, 6H, PCH_2), 1.02 (m, 9H, PCH_2CH_3)	220.5 (d, J(PC) = 30, CO), 213.9 (CO), 107.0 (br, cage C), 26.3 (SMe), 16.4 (d, J(PC) = 29, PCH_2), 10.2 (br, PCH_2CH_3)
11	7.29 (br s, 1H, cage CH), 1.95 (m, 12H, CH_2), 1.02 (m, 18H, CH_3)	222.4 (d, J(PC) = 29, CO), 213.9 (CO), 109.1 (br, cage C), 20.4 (d, J(PC) = 28, PCH_2), 15.2 (d, J(PC) = 28, PCH_2), 8.1 (br, PCH_2CH_3), 6.7 (br, PCH_2CH_3)
12	6.72 (br, 1H, cage CH), 3.69 (br, 2H, OCH_2), 2.70 (br, 2H, CH_2), 2.52 (br, 2H, CH_2), 1.98 (m, 8H, PCH_2CH_3), 1.81 (br, 2H, CH_2), 1.25 (m, 12H, CH_3)	215.0 (CO), 213.6 (CO), 99.1 (br, cage C), 70.2 (OCH_2), 31.1 (CH_2), 25.6 (CH_2), 17.0 (d, J(PC) = 48, PCH_2), 11.7 (d, J(PC) = 49, PCH_2), 5.2 (br, PCH_2CH_3)

[a] Chemical shifts (δ) in ppm, coupling constants (J) in hertz, measurements at ambient temperatures in CD_2Cl_2. [b] Resonances for terminal BH protons occur as broad unresolved signals in the range δ ca. −1 to +3. [c] ^{1}H-decoupled chemical shifts are positive to high frequency of $SiMe_4$.

Table 3. ^{11}B and ^{31}P NMR Data[a]

compd	chem shift	
	^{11}B[b]	^{31}P[c]
1a	36.8 (2B), 1.2 (2B), −17.8 (2B), −25.6	
2	16.2, 7.3 (2B), 0.8 (2B), −11.6 (2B)	
4	33.0 (2B), 0.1 (2B), −14.9 (2B), −31.5	8.2 (br)
5	12.6, 9.0 (2B), 0.2 (2B), −12.1 (2B)	7.8 (br)
6	34.1 (2B), 0.3 (2B), −15.2 (2B), −34.8	17.4 (vbr d, J(AgP) = ca. 650)
7	17.5, 10.6 (B(7)), 10.6, 4.9, 1.2, −10.7, −16.3	
8	32.9 (B(7)), 18.3, 10.3, 0.5 (2B), −8.9, −15.7	
9	15.2, 11.7, 10.3 (B(7)), 4.6, 3.3, −10.2, −16.4	
10	16.3, 13.0 (B(7)), 9.3, 3.3, 0.7, −10.9, −16.3	54.2 (s, Fe−PEt_3)
11	13.7, 8.9, 8.0, 1.7, −0.1 (d, J(PB) = ca. 106, B(7)), −12.2, −12.9	52.4 (s, Fe−PEt_3), 9.4 (q, J(BP) = ca. 109, B−PEt_3)
12	31.2 (B(7)), 23.6, 10.2, 1.2 (2B), −8.5, −12.5	38.8

[a] Chemical shifts (δ) in ppm, coupling constants (J) in hertz, measurements at ambient temperatures in CD_2Cl_2. [b] ^{1}H-decoupled chemical shifts are positive to high frequency of $BF_3{\cdot}OEt_2$ (external); resonances are of unit integral except where indicated. [c] ^{1}H-decoupled chemical shifts are positive to high frequency of 85% H_3PO_4 (external). Compounds **1a** and **2** additionally show a singlet at δ 21.7 for the $[N(PPh_3)_2]^+$ cation.

added to facilitate removal of the carbonyl ligands. Interestingly, although the same protocol was applied to **1a** and **2**, no CO substitution was achieved, even in refluxing THF.

The ^{11}B NMR spectrum for **1a** shows a set of four resonances in the ratio 2:2:2:1 (low to high field), while for **2** there are also four signals, with respective intensity ratio 1:2:2:2. Both of these patterns parallel the mirror symmetry evidenced by the X-ray diffraction studies. A single resonance for the CO groups is seen at δ 215.3 in the $^{13}C\{^{1}H\}$ NMR spectrum of **1a**, while for **2** there are two such signals (δ 214.5 and 213.8) for the CO ligands bonded to two different iron centers. The cage {CH} units in the two clusters have very distinctly different NMR characteristics: in **1a** this group gives rise to a signal at δ 3.68 in the ^{1}H NMR spectrum and at δ 32.3 in the $^{13}C\{^{1}H\}$ NMR spectrum, both of these chemical shifts being quite typical for such atoms.[16] For compound **2**, the {CH} vertex appears significantly deshielded compared with **1a**, with the corresponding parameters being δ 7.06 (^{1}H) and 105.2 (^{13}C). It appears that these chemical shift differences are characteristic for the {CH} unit in 9- versus 10-vertex clusters.

Notwithstanding the above observations regarding the apparent stability of the 6,10,1-Fe_2CB_7 architecture in **2**, there is some evidence that the anion can undergo chemically induced rearrangement, an intriguing possibility that we continue to investigate. However, this is complicated by the fact that—not surprisingly—the anion of **2** is also quite sensitive to protonation, especially in the presence of traces of water. Mixtures containing several products with various (multiple) degrees of B−OH substitution were observed in these reactions, preliminary identification of these species being via NMR spectroscopic evidence and X-ray diffraction studies. Further studies upon these transformations also are ongoing, and we hope to report further in due course. Unfortunately in these experiments a stable, clearly defined product where one or both of the metal centers in **2** became protonated was not obtained.

(16) Brew, S. A.; Stone, F. G. A. *Adv. Organomet. Chem.* **1993**, *35*, 135.

Chart 3

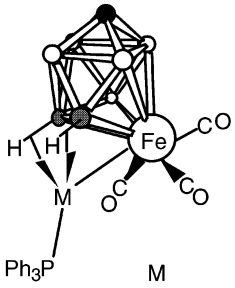

M

4 Cu
6 Ag

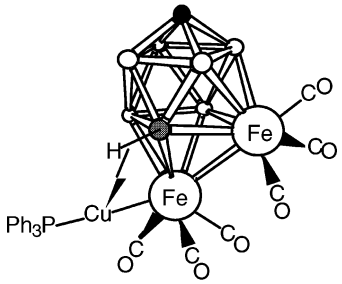

5

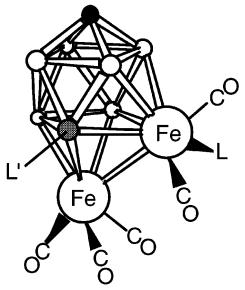

	L	L'
7	CO	SMe_2
8	CO	THF
9	SMe_2	SMe_2
10	PEt_3	SMe_2
11	PEt_3	PEt_3
12	CO	$O(CH_2)_4PEt_3$

○ BH ◍ B ● CH

Alternatively, however, since the fragments {M(PPh$_3$)}$^+$ (M = Cu, Ag) are isolobal with the proton,[17] it seemed likely that these cations would react with **1a** and **2** to afford bi- and trimetallic clusters, respectively, similar to the reactions of the same cations with **3**.[18] Accordingly, treatment of **1a** or **2** in THF with [CuCl(PPh$_3$)]$_4$, with Tl[PF$_6$] added to remove chloride as insoluble TlCl (cage:Cu:Tl ratio 1:1:1), yielded the heterometallic compounds [6,7,9-{Cu(PPh$_3$)}-6,9-(μ-H)$_2$-7,7,7-(CO)$_3$-*closo*-7,1-FeCB$_7$H$_6$] (**4**) and [7,10-{Cu(PPh$_3$)}-7-(μ-H)-6,6,6,10,10,10-(CO)$_6$-*closo*-6,10,1-Fe$_2$CB$_7$H$_7$] (**5**), respectively (Chart 3). The Ag analogue of **4**, namely [6,7,9-{Ag(PPh$_3$)}-6,9-(μ-H)$_2$-7,7,7-(CO)$_3$-*closo*-7,1-FeCB$_7$H$_6$] (**6**), was obtained similarly from **1a**, Ag[BF$_4$], and PPh$_3$, but the corresponding AgFe$_2$ derivative of **2** could not be obtained by the same route. Instead, the anion of compound **2**, upon reaction with Ag[BF$_4$] and PPh$_3$, gave a mixture of compounds **1b** and **6**, identified both structurally and spectroscopically.

Evidently, addition of the silver cation results in an excision of one iron vertex from the cluster of **2**, a reverse of the formation of **2** from **1a**. The silver-promoted reaction likely involves oxidation of an iron center and thus conceivably weakens its bonding with the rest of the cluster. Surprisingly, this reaction does not occur with Ag[BF$_4$] in the absence of PPh$_3$, and it may be that the phosphine is involved in stabilizing an intermediate or that the {Ag(PPh$_3$)}$^+$ moiety first binds to the diferracarborane prior to reaction with further silver to remove one iron vertex. The demetalation reaction is apparently also solvent dependent. Thus, in CH_2Cl_2 the anion of **1** was not obtained, but instead only B-hydroxylated species akin to those just mentioned were observed. In THF, however, the conversion to the monoiron species is achieved, further suggesting the necessity of coordinative stabilization of an intermediate. In practice, a 1:1 mixture of THF and CH_2Cl_2 was the preferred medium for this reaction, to avoid the additional complication of solvent polymerization that was noted in neat THF. The latter phenomenon may be catalyzed by traces of H[BF$_4$] formed from the hygroscopic Ag[BF$_4$] reagent and adventitious water.

The structures of all of compounds **1b** and **4**−**6** were established by X-ray diffraction studies: that of **1b** has already been discussed above. In Figure 2 the structures of **4** and **6** are compared. The presence of pendant {M(PPh$_3$)} substituents on the FeCB$_7$ framework is clearly evident (B(6)···Cu(1) = 2.150(2) Å and B(9)···Cu(1) = 2.122(2) Å in **4**; B(6)···Ag(1) = 2.505(2) Å and B(9)···Ag(1) = 2.337(2) Å in **6**). In addition, the exo-polyhedral atom M forms a direct M−Fe bond with the cluster Fe vertex (Fe(1)−Cu(1) = 2.7562(4) Å in **4**; Fe(1)−Ag(1) = 3.0419(4) Å in **6**). In Figure 3 is shown the structure of compound **5**. Again, a {Cu(PPh$_3$)} unit is appended to the {Fe$_2$CB$_7$} framework, with Fe(10)−Cu(1) = 2.5099(3) Å, and it may be of interest that the Fe−Cu bond involves the iron vertex in the 4-coordinate site. As noted above, the site of lower connectivity is general favored by more electronegative carbon vertexes. Conversely, this might imply that a 4-connected iron vertex would be more electron rich than a 5-coordinate one[12b] and, hence, the atom Fe(10) is a better donor for the exo-polyhedral copper center. The {BH(7)} group partakes in a supporting 3-center, 2-electron B−H⇀Cu bond with the exo-polyhedral unit (B(7)···Cu(1) = 2.1707(15) Å, H(7)−Cu(1) = 1.719(16) Å).

The spectroscopic parameters for **1b** and **4**−**6** are consistent with their solid-state structures. For **1b**, the room-temperature $^{31}P\{^1H\}$ NMR spectrum showed a singlet at δ 11.8 that is assigned to the [Ag(PPh$_3$)$_3$]$^+$ group. This may be compared with literature NMR data (at 193 K) of δ 11.5, with $J(^{107}Ag^{31}P)$ and $J(^{109}Ag^{31}P)$ coupling constants of 319 and 367 Hz,[19] and the absence of Ag−P coupling in the present case may be suggestive of some phosphine exchange at ambient temperatures, perhaps even involving loose interactions between silver and the anion. The ^{1}H NMR spectrum showed a broad

(17) Stone, F. G. A. *Angew. Chem., Int. Ed. Engl*. **1984**, *23*, 89.
(18) Ellis, D. D.; Franken, A.; Jelliss, P. A.; Kautz, J. A.; Stone, F. G. A.; Yu, P.-Y. *Dalton Trans*. **2000**, 2509.
(19) Alyea, E. C.; Malito, J.; Nelson, J. H. *Inorg. Chem.* **1987**, *26*, 4294.

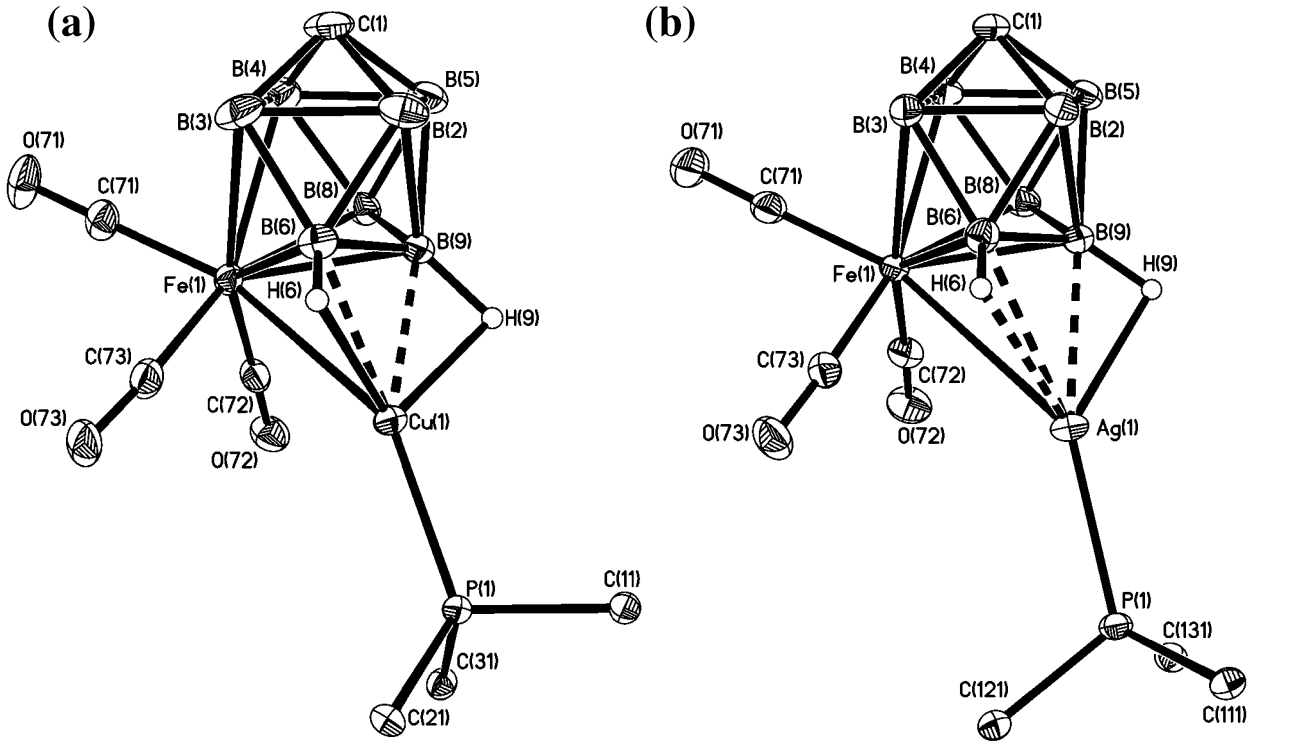

Figure 2. Perspective view of one of the crystallographically independent molecules of compounds (a) **4** and (b) **6**, showing the crystallographic labeling schemes. Selected internuclear distances (Å) and interbond angles (deg) are as follows. For **4**: Fe(1)−Cu(1) = 2.7562(4), Fe(1)−B(3) = 2.311(2), Fe(1)−B(4) = 2.347(2), Fe(1)−B(6) = 2.098(2), Fe(1)−B(8) = 2.110(2), Fe(1)−B(9) = 2.250(2), B(3)···B(4) = 2.129(3), B(6)···Cu(1) = 2.150(2), Cu(1)−H(6) = 2.03(2), B(9)···Cu(1) = 2.122(2), Cu(1)−H(9) = 1.85(2); P(1)−Cu(1)−Fe(1) = 145.689(17). For **6**: Fe(1)−Ag(1) = 3.0419(4), Fe(1)−B(3) = 2.307(2), Fe(1)−B(4) = 2.349(2), Fe(1)−B(6) = 2.101(2), Fe(1)−B(8) = 2.101(2), Fe(1)−B(9) = 2.282(2), B(3)···B(4) = 2.138(3), B(6)···Ag(1) = 2.505(2), Ag(1)−H(6) = 2.44(3), B(9)···Ag(1) = 2.337(2), Ag(1)−H(9) = 2.04(3); P(1)−Ag(1)−Fe(1) = 140.768(15). In the other crystallographically independent molecule of each compound, the Cu or Ag is closer to the Fe (Fe(1A)−Cu(1A) is 2.6785(5) Å; Fe(1A)−Ag(1A) is 2.8766(5) Å) and more distant from BH(6) (B(6A)···Cu(1A) = 2.178(2), B(9A)···Cu(1A) = 2.119(2); B(6A)···Ag(1A) = 2.596(2), B(9A)···Ag(1A) = 2.338(2) Å).

multiplet (δ 7.48−7.08) for the phenyl protons plus a broad singlet (δ 2.85) for the cage CH, with these being in the ratio 45:1, further confirming the constitution of the cation. All other data for the anion were similar to those of **1a**.

Data for compounds **4**−**6** are presented in Tables 1−3. In the $^{11}B\{^1H\}$ NMR spectra of all three species, four resonances are observed, in the respective ratios 2:2:2:1 (**4** and **6**) and 1:2:2:2 (**5**). Their chemical shifts are very similar to, but slightly more shielded than, those for the parent anions. The integral ratios imply mirror-symmetric structures that are at odds with those determined in the solid state. However, it is highly likely that the exo-polyhedral $\{M(PPh_3)\}$ unit is fluxional, so that the molecule appears symmetric on the NMR time scale. Likewise, such processes mean that no signals for protons involved in B−H→M bridges are seen in the ^1H NMR spectra.[20,21] The $^{31}P\{^1H\}$ NMR spectra of **4** and **5** show broad resonances at δ 8.2 (**4**) and 7.8 (**5**) that may be assigned to their $\{Cu(PPh_3)\}$ groups: these peaks are broadened by unresolved coupling to quadrupolar boron and copper nuclei. For **6**, a very broad doublet centered at δ 17.4 is seen, with an approximate Ag−P coupling constant of 650 Hz. Individual $J(^{107}Ag^{31}P)$ and $J(^{109}Ag^{31}P)$ values could not be resolved.

It may be noted in passing that, surprisingly, no complexes analogous to compounds **4**−**6** were obtained by treatment of **2** with $[AuCl(PPh_3)]$ in THF in the presence of $Tl[PF_6]$. Instead, the reaction apparently leads to degradation of the metallacarborane cage, and no identifiable products could be isolated.

As noted above, replacement of the CO groups in **1a** and **2** by donor molecules proved to be far more difficult than in the anion **3**, and even in the presence of Me_3NO at elevated temperatures no replacement of a CO group occurred. It is known[15,22] that a decrease in Fe−CO bond strength in such species may be achieved by conversion to a neutral, zwitterionic species. Typically, in earlier studies the anion **3** was shown to undergo hydride abstraction by reaction with strong acids in the presence of donors L to give the charge-compensated compounds $[7\text{-L-}2,2,2\text{-}(CO)_3\text{-}closo\text{-}2,1\text{-}FeCB_{10}H_{10}]$.[15,22] The anion of **1a** did not undergo a similar kind of reaction, but with **2** substitution was achieved. Thus, compound **2**, dissolved in neat SMe_2, after addition of CF_3SO_3H afforded the B-substituted complex $[6,6,6,10,10,10\text{-}(CO)_6\text{-}7\text{-}SMe_2\text{-}closo\text{-}6,10,1\text{-}$

(20) Long, J.; Marder, T. B.; Behnken, P. E.; Hawthorne, M. F. *J. Am. Chem. Soc*. **1984**, *106*, 2979.

(21) (a) Jeffrey, J. C.; Ruiz, M. A.; Sherwood, P.; Stone, F. G. A. *J. Chem. Soc., Dalton Trans.* **1989**, 1845. (b) Carr, N.; Gimeno, M. C.; Goldberg, J. E.; Pilotti, M. U.; Stone, F. G. A.; Topaloglu, I. *J. Chem. Soc., Dalton Trans.* **1990**, 2253. (c) Jeffery, J. C.; Jelliss, P. A.; Stone, F. G. A. *J. Chem. Soc., Dalton Trans*. **1993**, 1073. (d) Jeffery, J. C.; Jelliss, P. A.; Rees, L. H.; Stone, F. G. A. *Organometallics* **1998**, *17*, 2258.

(22) Franken, A.; Du, S.; Jelliss, P. A.; Kautz, J. A.; Stone, F. G. A. *Organometallics* **2001**, *20*, 1597.

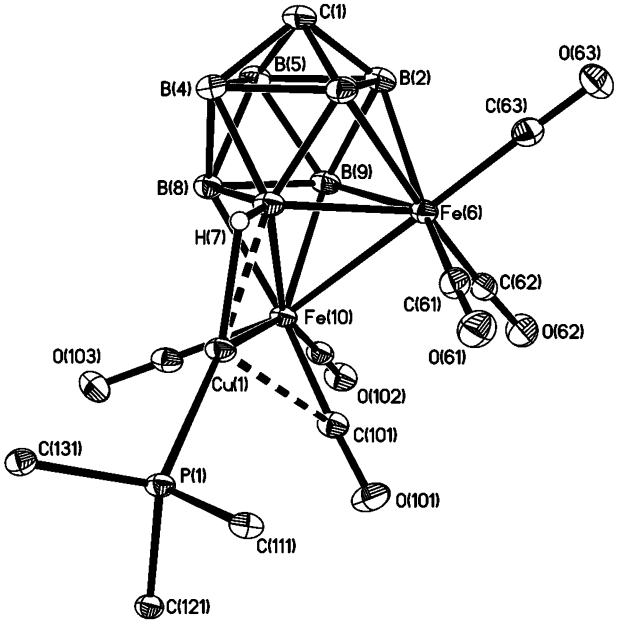

Figure 3. Structure of compound **5**, showing the crystallographic labeling scheme. Selected internuclear distances (Å) and interbond angles (deg): Fe(6)−Fe(10) = 2.5676(3), Fe(6)−B(2) = 2.1799(16), Fe(6)−B(3) = 2.1603(15), Fe(6)−B(7) = 2.2216(16), Fe(6)−B(9) = 2.2401(16), Fe(10)−B(7) = 2.1920(15), Fe(10)−B(8) = 2.1156(15), Fe(10)−B(9) = 2.1957(14), Fe(10)−Cu(1) = 2.5099(3), B(7)···Cu(1) = 2.1707(15), Cu(1)−H(7) = 1.719(16), Cu(1)−P(1) = 2.2170(4), Cu(1)···C(101) = 2.4142(13), B(2)···B(3) = 1.969(2); Cu(1)−Fe(10)−Fe(6) = 90.592(11), O(101)−C(101)−Fe(10) = 172.68(12), B(7)−Cu(1)−P(1) = 164.39(4), P(1)−Cu(1)−Fe(10) = 140.322(12).

$Fe_2CB_7H_7$] (**7**) in almost quantitative yield. Similarly, addition of CF_3SO_3H to **2** in CH_2Cl_2−THF (1:1) at 0 °C gave the complex [6,6,6,10,10,10-$(CO)_6$-7-{$O(CH_2)_4$}-*closo*-6,10,1-$Fe_2CB_7H_7$] (**8**), also in excellent yield.

Data characterizing compounds **7** and **8** are listed in Tables 1−3. In their IR spectra (Table 1) strong CO stretching bands are observed at 2063, 2023, and 1996 cm^{-1} (**7**) and at 2062, 2021, and 1992 cm^{-1} (**8**). These values are almost 30 cm^{-1} higher than the values that are observed for the starting material **2**. The $^{11}B\{^1H\}$ NMR spectra of both **7** and **8** display seven separate resonances, indicating a loss of mirror symmetry upon cage substitution. Of these peaks, one resonance, at δ 10.6 for **7** and at δ 32.9 for **8**, remained a singlet in a fully coupled ^{11}B spectrum and this may be assigned to the B−L nucleus. In addition, peaks are seen in the ^1H and $^{13}C\{^1H\}$ NMR spectra in typical positions for the pendant SMe_2 and THF moieties. A preliminary comparison of the ^{11}B NMR peak positions for **7** and **8** versus those for **2** suggested that the site of B−L substitution is at B(7). This proposal is reasonable, given that this vertex is bonded to both metal atoms, is distant from the carbon vertex, and therefore would be expected to have carried the most hydridic H atom. Indeed, this was confirmed by an X-ray diffraction study of **7**, the results of which are included as Supporting Information. The structure of compound **9** discussed below also corroborates these findings.

The enhanced reactivity of the CO groups in compound **7** toward substitution was demonstrated by dissolving **7** in neat SMe_2 and adding Me_3NO. Upon addition of the latter an immediate color change was observed and the compound [6,6,10,10,10-$(CO)_5$-6,7-$(SMe_2)_2$-*closo*-6,10,1-$Fe_2CB_7H_7$] (**9**) was formed. Perhaps surprisingly, the CO ligands in **7** still could not be replaced without facilitation by Me_3NO. Data characterizing **9** are listed in Tables 1−3. The presence of the SMe_2 substituent on an iron center causes the three CO stretching bands in the IR spectrum to be lowered by almost 30 cm^{-1} compared to those in **7**. Like the parent species **7**, the $^{11}B\{^1H\}$ NMR spectrum of compound **9** also displayed a set of seven resonances, of which one (at δ 10.3) remained a singlet upon retention of proton coupling and hence may be assigned to the B−SMe_2 nucleus.

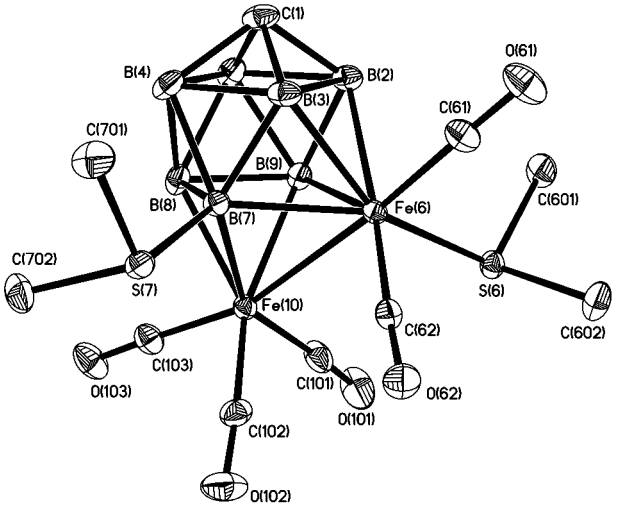

Figure 4. Perspective view of the structure of compound **9**, showing the crystallographic labeling scheme. Selected internuclear distances (Å) and interbond angles (deg): Fe(6)−Fe(10) = 2.5683(14), Fe(6)−B(2) = 2.166(2), Fe(6)−B(3) = 2.152(2), Fe(6)−B(7) = 2.192(2), Fe(6)−B(9) = 2.238(2), Fe(6)−S(6) = 2.2902(10), Fe(10)−B(7) = 2.152(2), Fe(10)−B(8) = 2.087(2), Fe(10)−B(9) = 2.177(2), B(2)···B(3) = 2.001(3), B(7)−S(7) = 1.929(2); S(6)−Fe(6)−Fe(10) = 96.33(2).

To confirm the positions of the iron- and boron-bound SMe_2 ligands, an X-ray diffraction study of compound **9** was deemed worthwhile. The molecule is shown in Figure 4. One of the CO groups on Fe(6) (notably, the iron atom with cluster connectivity 5) is replaced by an SMe_2 ligand (Fe(6)−S(6) = 2.2902(10) Å), and the second such moiety is bonded to B(7) (B(7)−S(7) = 1.929(2) Å), which is adjacent to both Fe(6) and Fe(10). The distance Fe(6)−Fe(10) (2.5683(14) Å) is somewhat longer than that (2.5512(4) Å) in **2** and in fact is rather closer to the corresponding separation (2.5676(3) Å) in **5**, which formally may also be considered a charge-compensated species.

Attempts to prepare derivatives analogous to **9** by treatment of **7** with other ligands L in the presence of Me_3NO met with very limited success. An apparent related product was isolated with L = $CNC_6H_3Me_2$-2,6, but this was very unstable and thus defied complete characterization. With L = PPh_3 or $Bu^tC{\equiv}CH$, even greater instability was encountered and the only identifiable carborane-containing species formed was the anion [*closo*-2-CB_6H_7]$^-$, identified by ^{11}B NMR.[7a,23]

When **7** was treated with PEt_3 in the presence of Me_3NO, initial substitution of an Fe-bound carbonyl

ligand occurs to give a moderately stable product that could be isolated after a reaction time of ca. 30 min, and which was tentatively identified as [6,6,10,10,10-$(CO)_5$-7-SMe_2-6-PEt_3-*closo*-6,10,1-$Fe_2CB_7H_7$] (**10**). The same reaction, using excess PEt_3 and with a reaction time of 18 h, afforded [6,6,10,10,10-$(CO)_5$-6,7-$(PEt_3)_2$-*closo*-6,-10,1-$Fe_2CB_7H_7$] (**11**), apparently formed via **10** with subsequent displacement of the boron-bound SMe_2 unit by a second PEt_3 ligand. (Spectroscopic monitoring of the reaction mixture supported the proposed sequence.) These reactions are not clean, however, and isolation of **10** is complicated by its ready conversion to **11**. Notwithstanding this, spectroscopic data (Tables 2 and 3) reasonably identified the two species. Substitution of a metal-bound CO by PEt_3 is evidenced by the lowering of CO stretching frequencies upon conversion of **7** to **10**. In addition, ^1H and $^{13}C\{^1H\}$ NMR data for **10** and **11** show the successive appearance of one and then two PEt_3 ligands, with appropriate integrals (^1H NMR) relative to the SMe_2 and/or cage CH units, and the absence of an SMe_2 ligand in **11**. In the $^{31}P\{^1H\}$ NMR spectrum of **10** is seen a singlet at δ 54.2, assigned to an Fe-bound PEt_3, with a similar peak appearing at δ 52.4 in the spectrum of **11**. Crucially, the latter spectrum also shows a second 1:1:1:1 quartet resonance at δ 9.4 (J(BP) = ca. 109 Hz) characteristic of phosphorus bound to boron, with a corresponding doublet in the $^{11}B\{^1H\}$ NMR spectrum at δ −0.1 (J(PB) = ca. 106 Hz). All other signals in the latter spectrum become doublets upon retention of proton coupling, confirming loss of SMe_2, while the sulfur ligand is clearly still present in **10**, giving rise to a singlet at δ 13.0 in the fully coupled ^{11}B spectrum.

In contrast to the above reaction sequence, treatment of compound **8** in CH_2Cl_2 with PEt_3 gives a different type of charge-compensated species, namely [6,6,6,10,10,10-$(CO)_6$-7-{$O(CH_2)_4PEt_3$}-*closo*-6,10,1-$Fe_2CB_7H_7$] (**12**). In the latter, the formal positive charge that formerly was located on the THF oxygen atom is now located on the phosphorus center. Formation of **10** involves nucleophilic attack by the PEt_3 ligand, resulting in cleavage of a C−O bond in the THF group, and is similar in character to reactions observed earlier in related systems.[24] The pattern of chemical shifts displayed in the $^{11}B\{^1H\}$ NMR spectrum is very similar to compound **9**, with a resonance at δ 31.2 which remained a singlet in the fully coupled ^{11}B spectrum and which may be assigned to the B−$O(CH_2)_4PEt_3$ nucleus. In the ^1H NMR spectrum, four separate integral 2 multiplets are seen for the four CH_2 units of the pendant $O(CH_2)_2PEt_3$ group, at δ 3.69, 2.70, 2.52, and 1.81, with four corresponding signals (δ 70.2, 31.1, 25.6, 11.7) in the $^{13}C\{^1H\}$ NMR spectrum. Of the latter, the last is a doublet (J(PC) = 49 Hz) due to the adjacent phosphorus center.

Conclusion

Several interesting results stem from the studies described herein. The smaller carborane [*closo*-1-$CB_7H_8]^-$ has been demonstrated readily to undergo a cage-opening reaction upon heating with $[Fe_3(CO)_{12}]$, inserting an {$Fe(CO)_3$} fragment, and giving the anion of compounds **1**. The latter itself undergoes a further oxidative insertion of {$Fe(CO)_3$} to afford the anion of **2**. In this the iron reagent shows a surprising level of nucleophilicity, with the boron-containing clusters likewise revealing unexpectedly facile closo → nido reductive cage opening. Whereas the anion **3**[15,22] reacts with donor molecules in the presence of Me_3NO, the anions of compounds **1** and **2** do not react under these conditions, as a result of the stronger bonding of their CO ligands to the iron centers. Nevertheless, CO substitution was achieved after **2** was converted to the charge-compensated complex **7**, with CO replacement occurring at the iron atom located in the higher coordinated position in the dimetallacarborane cluster. The removal of an {$Fe(CO)_3$} fragment from the anion of **2** by simple oxidation using Ag^+ also leads to the 9-vertex ferracarborane of compounds **1**, an observation which itself may lead to further useful chemistry.

Experimental Section

General Considerations. All reactions were carried out under an atmosphere of dry, oxygen-free dinitrogen using Schlenk line techniques. Solvents were stored over and distilled from appropriate drying agents under dinitrogen prior to use. Petroleum ether refers to that fraction of boiling point 40−60 °C. Chromatography columns (typically ca. 15 cm in length and ca. 2 cm in diameter) were packed with silica gel (Acros, 60−200 mesh). Filtration through Celite typically employed a plug ca. 5 cm long and ca. 2 cm in diameter. NMR spectra were recorded at the following frequencies (MHz): ^1H, 360.1; ^{13}C, 90.6; ^{11}B, 115.5; ^{31}P, 145.8. The compounds $[NBu^n_4]$[*closo*-1-CB_7H_8][7b] and $[CuCl(PPh_3)]_4$[25] were prepared according to the literature; all other materials were used as received.

Synthesis of $[N(PPh_3)_2][7,7,7\text{-}(CO)_3$-*closo*-$7,1\text{-}FeCB_7H_8]$ and $[N(PPh_3)_2][6,6,6,10,10,10\text{-}(CO)_6$-*closo*-$6,10,1\text{-}Fe_2CB_7H_8]$. The compounds $[Fe_3(CO)_{12}]$ (0.50 g, 1.0 mmol) and $[NBu^n_4]$[*closo*-1-CB_7H_8] (0.34 g, 1.0 mmol) were heated to reflux in THF (10 mL) for 18 h. The resulting mixture was cooled to room temperature, and $[N(PPh_3)_2]Cl$ (0.58 g, 1.0 mmol) was added. Solvent was removed in vacuo, the residue was dissolved in CH_2Cl_2 (2 mL), and this solution was transferred to the top of a chromatography column. Elution with CH_2Cl_2−petroleum ether (4:1) gave successively a red fraction followed by an orange fraction. Removal of solvent in vacuo from the two fractions yielded, respectively, red microcrystals of $[N(PPh_3)_2]$[6,6,6,10,10,10-$(CO)_6$-*closo*-6,10,1-$Fe_2CB_7H_8$] (**2**; 0.29 g) and orange microcrystals of $[N(PPh_3)_2]$[7,7,7-$(CO)_3$-*closo*-7,1-$FeCB_7H_8$] (**1a**; 0.13 g).

Analysis (^{11}B NMR) of the above reaction mixture after only 5 h at reflux temperature indicated that at this point the main product was the anion of compound **1a**, along with some unreacted carborane. The metallacarborane could be isolated at this point in ca. 47% yield. Compound **1a**, upon further treatment with excess $[Fe_3(CO)_{12}]$, was converted essentially quantitatively to **2** (63% isolated yield).

Attempts to prepare the same ferracarboranes using [Fe-$(CO)_5$] or $[Fe_2(CO)_9]$ as the iron reagents met with mixed success. With the former, final yields of **1a** and **2** were slightly lower, and product contamination was slightly worse, than when $[Fe_3(CO)_{12}]$ was used, whereas with $[Fe_2(CO)_9]$ yields were very poor indeed. For these reasons the dodecacarbonyl was the substrate of choice for this synthesis.

(23) Stíbr, B.; Tok, O. L.; Milius, W.; Bakardjiev, M.; Holub, J.; Hnyk, D.; Wrackmeyer, B. *Angew. Chem., Int. Ed.* **2002**, *41*, 2126.

(24) Mullica, D. F.; Sappenfield, E. L.; Stone, F. G. A.; Woollam, S. F. *Organometallics* **1994**, *13*, 157. Gómez-Saso, M.; Mullica, D. F.; Sappenfield, E.; Stone, F. G. A. *Polyhedron* **1996**, *15*, 793. Du, S.; Franken, A.; Jelliss, P. A.; Kautz, J. A.; Stone, F. G. A.; Yu, P.-Y. *Dalton Trans.* **2001**, 1846.

(25) Jardine, F. H.; Rule, J.; Vohra, G. A. *J. Chem. Soc. A* **1970**, 238.

Table 4. Crystallographic Data for 1b, 2, 4−6, and 9[a]

	1b	2	4	5	6	9
formula	$C_{58}H_{53}AgB_7FeO_3P_3$	$C_{43}H_{38}B_7Fe_2NO_6P_2$	$C_{22}H_{23}B_7CuFeO_3P$	$C_{25}H_{23}B_7CuFe_2O_6P$	$C_{22}H_{23}AgB_7FeO_3P$	$C_{10}H_{19}B_7Fe_2O_5S_2$
fw	1130.30	914.05	561.43	701.31	605.76	470.74
space group	$P\bar{1}$	$P2_1/c$	$P2_1/c$	$P\bar{1}$	$P\bar{1}$	$P\bar{1}$
a, Å	11.4489(7)	16.6125(19)	14.9313(18)	10.3282(8)	10.5912(13)	8.002(4)
b, Å	13.3757(8)	13.5446(17)	15.151(2)	12.3809(9)	12.0247(14)	8.815(5)
c, Å	19.6269(12)	19.846(3)	22.761(3)	13.1265(10)	22.158(3)	15.159(8)
α, deg	86.029(3)	90	90	69.200(4)	94.682(6)	84.306(13)
β, deg	75.552(2)	105.643(6)	103.502(5)	85.465(4)	99.077(6)	82.306(12)
γ, deg	67.204(2)	90	90	65.840(3)	113.080(6)	67.586(13)
V, Å^3	2681.9(3)	4300.2(9)	5006.8(11)	1427.35(19)	2531.4(5)	978.3(9)
Z	2	4	8	2	4	2
ρ_{calcd}, g cm^{-3}	1.400	1.412	1.490	1.632	1.589	1.598
μ(Mo Kα), mm^{-1}	0.770	0.798	1.517	1.837	1.433	1.713
no. of rflns measd	60 120	77 031	53 137	31 959	59 014	17 182
no. of indep rflns	16 713	16 086	15 519	8884	17 625	6339
R_{int}	0.0349	0.0390	0.0418	0.0271	0.0249	0.0307
wR2, R1[b] (all data)	0.0818, 0.0433	0.1142, 0.0609	0.0866, 0.0598	0.0725, 0.0354	0.0810, 0.0387	0.0822, 0.0455
wR2, R1 (obsd[c] data)	0.0790, 0.0316	0.1056, 0.0401	0.0771, 0.0370	0.0700, 0.0266	0.0783, 0.0330	0.0757, 0.0337

[a] For all determinations, T = 110(2) K. [b] wR2 = $[\sum\{w(F_o^2 - F_c^2)^2\}/\sum w(F_o^2)^2]^{1/2}$; R1 = $\sum||F_o| - |F_c||/\sum|F_o|$. [c] $F_o > 4\sigma(F_o)$.

Synthesis of [6,7,9-{Cu(PPh$_3$)}-6,9-(μ-H)$_2$-7,7,7-(CO)$_3$-*closo*-7,1-FeCB$_7$H$_6$]. Compound **1a** (0.20 g, 0.25 mmol), [CuCl(PPh$_3$)]$_4$ (0.09 g, 0.06 mmol), and Tl[PF$_6$] (0.09 g, 0.26 mmol) were stirred in THF (10 mL) at room temperature for ca. 18 h. The mixture was filtered (Celite) and the filtrate evaporated in vacuo. The residue was dissolved in CH_2Cl_2 (2 mL), and this solution was transferred to the top of a chromatography column. Elution with CH_2Cl_2−petroleum ether (1:1) gave an orange fraction. Removal of solvent in vacuo followed by crystallization from CH_2Cl_2−petroleum ether yielded red microcrystals of [6,7,9-{Cu(PPh$_3$)}-6,9-(μ-H)$_2$-7,7,7-(CO)$_3$-*closo*-7,1-FeCB$_7$H$_6$] (**4**; 0.13 g).

Synthesis of [Ag(PPh$_3$)$_3$][7,7,7-(CO)$_3$-*closo*-7,1-FeCB$_7$H$_8$] and [6,7,9-{Ag(PPh$_3$)}-6,9-(μ-H)$_2$-7,7,7-(CO)$_3$-*closo*-7,1-FeCB$_7$H$_6$]. The compounds **2** (0.46 g, 0.5 mmol), Ag[BF$_4$] (ca. 0.1 g, 0.5 mmol), and PPh$_3$ (0.13 g, 0.5 mmol) were stirred in CH_2Cl_2−THF (10 mL) at room temperature for ca. 18 h. After filtration of the mixture (Celite), the filtrate was evaporated in vacuo. The residue was dissolved in CH_2Cl_2 (2 mL), and this solution was applied to a chromatography column. Elution with CH_2Cl_2−petroleum ether (1:1) gave first an orange fraction, from which was obtained, after removal of solvent in vacuo and crystallization from CH_2Cl_2−petroleum ether, orange microcrystals of [6,7,9-{Ag(PPh$_3$)}-6,9-(μ-H)$_2$-7,7,7-(CO)$_3$-*closo*-7,1-FeCB$_7$H$_6$] (**6**; 0.18 g). Further elution with CH_2Cl_2−petroleum ether (4:1) gave another orange fraction, from which was similarly obtained orange microcrystals of [Ag(PPh$_3$)$_3$][7,7,7-(CO)$_3$-*closo*-7,1-FeCB$_7$H$_8$] (**1b**; 0.16 g, 29%).

Synthesis of [7,10-{Cu(PPh$_3$)}-7-(μ-H)-6,6,6,10,10,10-(CO)$_6$-*closo*-6,10,1-Fe$_2$CB$_7$H$_7$]. Similar to the synthesis of **4**, reaction of compound **2** (0.46 g, 0.50 mmol), [CuCl(PPh$_3$)]$_4$ (0.18 g, 0.12 mmol), and Tl[PF$_6$] (0.18 g, 0.52 mmol) in CH_2Cl_2 (10 mL), followed by an identical workup procedure, gave orange microcrystals of [7,10-{Cu(PPh$_3$)}-7-(μ-H)-6,6,6,10,10,10-(CO)$_6$-*closo*-6,10,1-Fe$_2$CB$_7$H$_7$] (**5**; 0.29 g).

Synthesis of [6,6,6,10,10,10-(CO)$_6$-7-L-*closo*-6,10,1-Fe$_2$CB$_7$H$_7$] (L = SMe$_2$, THF). (i) Compound **2** (0.46 g, 0.5 mmol) was dissolved in Me_2S (10 mL), CF_3SO_3H (0.25 mL) was added, and the mixture was stirred at room temperature for ca. 3 h. Solvent was evaporated in vacuo, the residue was dissolved in CH_2Cl_2 (2 mL), and this solution was transferred to the top of a chromatography column. Elution with CH_2Cl_2−petroleum ether (1:1) gave an orange fraction. Removal of solvent in vacuo, followed by crystallization from CH_2Cl_2−petroleum ether, yielded orange microcrystals of [6,6,6,10,10,10-(CO)$_6$-7-SMe$_2$-*closo*-6,10,1-Fe$_2$CB$_7$H$_7$] (**7**; 0.21 g).

(ii) Similarly, compound **2** (0.46 g, 0.5 mmol), treated with CF_3SO_3H (0.25 mL) in CH_2Cl_2−THF (1:1, 20 mL) at room temperature for ca. 6 h, with workup as above, yielded red microcrystals of [6,6,6,10,10,10-(CO)$_6$-7-{O(CH$_2$)$_4$}-*closo*-6,10,1-Fe$_2$CB$_7$H$_7$] (**8**) (0.16 g).

Synthesis of [6,6,10,10,10-(CO)$_5$-6,7-(SMe$_2$)$_2$-*closo*-6,10,1-Fe$_2$CB$_7$H$_7$]. Compound **7** (0.22 g, 0.25 mmol) was dissolved in Me_2S (5 mL), Me_3NO (ca. 0.040 g, 0.5 mmol) was added, and the solution was stirred at room temperature for ca. 18 h. Solvent was removed in vacuo, the residue was dissolved in CH_2Cl_2−petroleum ether (1:1, 2 mL), and this solution was transferred to the top of a chromatography column. Elution with CH_2Cl_2−petroleum ether (3:2) gave a red fraction which, after removal of solvent in vacuo and crystallization from CH_2Cl_2−petroleum ether, yielded dark red microcrystals of [6,6,10,10,10-(CO)$_5$-6,7-(SMe$_2$)$_2$-*closo*-6,10,1-Fe$_2$CB$_7$H$_7$] (**9**; 0.17 g).

Synthesis of [6,6,10,10,10-(CO)$_5$-6-PEt$_3$-7-L-*closo*-6,10,1-Fe$_2$CB$_7$H$_7$] (L = SMe$_2$, PEt$_3$). (i) Compound **7** (0.13 g, 0.25 mmol) was dissolved in CH_2Cl_2 (10 mL), PEt_3 (1.7 mmol, 0.25 mL) was added, followed by Me_3NO (0.075 g, 1.0 mmol), and the mixture was stirred at ambient temperature for 30 min. Solvent was removed in vacuo, and the residue was dissolved in a small amount of CH_2Cl_2−petroleum ether (1:1) and transferred to a chromatography column. Elution with the same solvent mixture gave first a red fraction that was collected and, after removal of solvents in vacuo, yielded dark red microcrystals of [6,6,10,10,10-(CO)$_5$-7-SMe$_2$-6-PEt$_3$-*closo*-6,10,1-Fe$_2$CB$_7$H$_7$] (**10**; ca. 0.10 g, 76%). IR: ν_{max}(CO) 2035 s, 1969 s, 1913 w cm^{-1}.

(ii) The same procedure, but with a reaction time of 18 h, gave dark red microcrystals of [6,6,10,10,10-(CO)$_5$-6,7-(PEt$_3$)$_2$-*closo*-6,10,1-Fe$_2$CB$_7$H$_7$] (**11**; ca. 0.08 g, 55%). IR: ν_{max}(CO) 2031 s, 1965 s, 1911 w cm^{-1}.

Synthesis of [6,6,6,10,10,10-(CO)$_6$-7-{O(CH$_2$)$_4$PEt$_3$}-*closo*-6,10,1-Fe$_2$CB$_7$H$_7$]. To compound **8** (0.11 g, 0.25 mmol) in CH_2Cl_2 (20 mL) was added PEt_3 (0.25 mL), and the mixture was stirred at room temperature for ca. 18 h. Solvent was removed in vacuo, and the residue was dissolved in CH_2Cl_2−CH_3CN (4:1, 2 mL) and applied to a chromatography column. Elution with CH_2Cl_2−CH_3CN (4:1) gave a red fraction, from which removal of solvent yielded red microcrystals of [6,6,6,10,10,-10-(CO)$_6$-7-{O(CH$_2$)$_4$PEt$_3$}-*closo*-6,10,1-Fe$_2$CB$_7$H$_7$] (**12**; 0.12 g).

Structure Determinations. Experimental data for all determinations are presented in Table 4. X-ray intensity data were collected at 110(2) K on a Bruker-Nonius X8 APEX CCD area-detector diffractometer using Mo Kα X-radiation (λ = 0.71073 Å). Several sets of narrow data "frames" were collected at different values of θ, for various initial values of ϕ and ω, using 0.5° increments of ϕ or ω. The data frames were integrated using SAINT;[26] the substantial redundancy in data

(26) APEX 2, version 1.0; Bruker AXS, Madison, WI, 2003−2004.

allowed an empirical absorption correction (SADABS)[26] to be applied, based on multiple measurements of equivalent reflections.

All structures were solved using conventional direct methods[26,27] and refined by full-matrix least squares on all F^2 data using SHELXTL version 6.12,[27] with anisotropic thermal parameters assigned to all non-H atoms. The locations of the cage-carbon atoms were verified by examination of the appropriate internuclear distances and the magnitudes of their isotropic thermal displacement parameters. Cluster BH and CH hydrogen atoms, apart from those for **1b**, were allowed positional refinement; all other H atoms were set riding in calculated positions with fixed isotropic thermal parameters defined as $U_{iso}(H) = 1.2[U_{iso}(parent)]$ or $U_{iso}(H) = 1.5[U_{iso}(parent)]$ for methyl groups.

(27) SHELXTL, version 6.12; Bruker AXS, Madison, WI, 2001.

Crystals of both **4** and **6** contained two independent molecules per asymmetric fraction of the unit cell. These differed in the relative orientations of phosphine phenyl rings with, in addition, some small differences in the dispositions of the exopolyhedral fragments.

Acknowledgment. We thank the Robert A. Welch Foundation for support and the National Science Foundation Major Research Instrumentation Program (Grant No. CHE-0321214) for funds to purchase the Bruker-Nonius X8-APEX diffractometer.

Supporting Information Available: Full details of crystallographic analyses (including that for compound **7**) as a CIF file. This material is available free of charge via the Internet at http://pubs.acs.org.

OM050584J